Generalized Nonconvex Hyperspectral Anomaly Detection via Background Representation Learning with Dictionary Constraint

Quan Yu [1] Minru Bai [1]

[1]School of Mathematics, Hunan University

Abstract

Anomaly detection in the hyperspectral images, which aims to separate interesting sparse anomalies from backgrounds, is a significant topic in remote sensing. In this paper, we propose a generalized nonconvex background representation learning with dictionary constraint (GNBRL) model for hyperspectral anomaly detection. Unlike existing methods that use a specific nonconvex function for a low rank term, GNBRL uses **a class of nonconvex functions for both low rank and sparse terms simultaneously**, which can better capture the low rank structure of the background and the sparsity of the anomaly. In addition, GNBRL **simultaneously learns the dictionary and anomaly tensor** in a unified framework by imposing a three-dimensional correlated total variation constraint on the dictionary tensor to enhance the quality of representation. An **extrapolated** linearized alternating direction method of multipliers (ELADMM) algorithm is then developed to solve the proposed GNBRL model. Finally, a novel **coarse to fine two-stage framework** is proposed to enhance the GNBRL model by exploiting the nonlocal similarity of the hyperspectral data. Theoretically, we establish an **error bound** for the GNBRL model and show that this error bound can be superior to those of similar models based on Tucker rank. We prove that the sequence generated by the proposed ELADMM algorithm converges to a Karush-Kuhn-Tucker point of the GNBRL model. This is a challenging task due to the nonconvexity of the objective function. Experiments on hyperspectral image datasets demonstrate that our proposed method outperforms several state-of-the-art methods in terms of detection accuracy. Code at `https://github.com/quanyumath/CF2-GNBRL`.

Generalized nonconvex model with dictionary constraint

Our **GNBRL** model is formulated as:

$$\min_{\mathcal{A},\mathcal{L},\mathcal{S}} \underbrace{\sum_{u=1}^{3}\alpha_u \|\nabla_u \mathcal{A}\|_{\psi}}_{\text{dictionary constraint}} + \lambda_1 \|\mathcal{L}\|_{\underbrace{\psi}_{\text{generalized nonconvex}}} + \lambda_2 \|\mathcal{S}\|_{\ell^{\psi}_{F,1}} \quad (2)$$
$$\text{s.t. } \mathcal{X} = \mathcal{A} * \mathcal{L} + \mathcal{S}.$$

	Other Models	Our Method
Dictionary Construction	Utilizes prebuilt dictionaries	Simultaneous dictionary construction and anomaly detection
Nonconvex Approximation	Specific nonconvex approximation for low rank	Generalized nonconvex approximation for both low rank and sparsity

ELADMM Algorithm to solve GNBRL

Input: The tensor data $\mathcal{X}$, parameters $\{\alpha_u\}_{u=1}^{3}$, λ_1, λ_2, β.

While not converge do

Step 1. Update $\mathcal{S}^{t+1}$.

Step 2. Let $\hat{\mathcal{A}}^t = \mathcal{A}^t + \omega^t_{\mathcal{A}}\left(\mathcal{A}^t - \mathcal{A}^{t-1}\right)$.

Step 3. Update $\mathcal{A}^{t+1}$.

Step 4. Update $\mathcal{C}_u^{t+1}$.

Step 5. Let $\hat{\mathcal{L}}^t = \mathcal{L}^t + \omega^t_{\mathcal{L}}\left(\mathcal{L}^t - \mathcal{L}^{t-1}\right)$.

Step 6. Update $\mathcal{L}^{t+1}$.

Step 7. Update multipliers $\mathcal{T}_u^{t+1}$ and penalty parameters β_u^{t+1}.

Let $t := t+1$ and go to Step 1.

end while

Output: $\mathcal{S}^{t+1}$, $\mathcal{A}^{t+1}$, $\mathcal{L}^{t+1}$.

CF2 framework for GNBRL

- **Coarse stage:** A coarse anomaly $\tilde{\mathcal{S}}$ is obtained by applying the GNBRL model to the whole HSI.
- **Fine stage:** We first divide the whole HSI into N patches third order sub-tensors according to BM3D. Then we apply the GNBRL model to each sub-tensor to obtain $\hat{\mathcal{S}}^1_{patch}, \hat{\mathcal{S}}^2_{patch}, \ldots, \hat{\mathcal{S}}^N_{patch}$. Next, we divide $\tilde{\mathcal{S}}$ into N patches following the partitions employed in the current fine stage to obtain $\tilde{\mathcal{S}}^1_{patch}, \tilde{\mathcal{S}}^2_{patch}, \ldots, \tilde{\mathcal{S}}^N_{patch}$. Finally, we obtain $\mathcal{S}^{\star}$ by

$$\mathcal{S}^{\star,l}_{patch} = \begin{cases} \tilde{\mathcal{S}}^l_{patch}, & \text{if } \operatorname{gap}\left(\tilde{\mathcal{S}}^l_{patch}, \hat{\mathcal{S}}^l_{patch}\right) < \varrho, \\ \hat{\mathcal{S}}^l_{patch}, & \text{if } \operatorname{gap}\left(\tilde{\mathcal{S}}^l_{patch}, \hat{\mathcal{S}}^l_{patch}\right) \geq \varrho. \end{cases} \quad (3)$$

Theoretical results

Error bound: Let $\left(\mathcal{L}^{\natural}, \mathcal{S}^{\natural}\right)$ be the pair of true low rank and sparse tensors, and $(\mathcal{A}^{\star}, \mathcal{L}^{\star}, \mathcal{S}^{\star})$ be an optimal solution to the optimization problem (2). Assume that $\mathcal{A}^{\star}$ satisfies ψ-RTEC(s), $\mathcal{X} = \mathcal{A}^{\star} * \mathcal{L}^{\natural} + \mathcal{S}^{\natural}$, $\left\|\mathcal{L}^{\natural}\right\|_{\psi} \leq \|\mathcal{L}^{\star}\|_{\psi} := s$, and $\lambda_2 > \lambda_1 r \vartheta^{\psi}_{r,s}$ with $r = \min\{n_1, n_2\}$. Then we have

$$\psi\left(\left\|\mathcal{S}^{\natural} - \mathcal{S}^{\star}\right\|_F\right) \leq \left\|\mathcal{S}^{\natural} - \mathcal{S}^{\star}\right\|_{\ell^{\psi}_{F,1}} \leq \frac{2\lambda_2 \left\|\mathcal{S}^{\natural}\right\|_{\ell^{\psi}_{F,1}}}{\lambda_2 - \lambda_1 r \vartheta^{\psi}_{r,s}}, \quad (1)$$

where $\vartheta^{\psi}_{r,s}$ is a constant that depends on r, s, ψ.

The low rank property of $\mathcal{L}^{\natural}$ and the sparsity of $\mathcal{S}^{\natural}$ are both positively correlated with $\vartheta^{\psi}_{r,s}$ and $\left\|\mathcal{S}^{\natural}\right\|_{\ell^{\psi}_{F,1}}$, which, in turn, are positively related to the error bound. Thus, the lower the rank of $\mathcal{L}^{\natural}$ and the sparser $\mathcal{S}^{\natural}$ is, the smaller the error bound.

Convergence analysis: Let $\left\{\mathcal{S}^t, \mathcal{A}^t, \mathcal{C}^t_u, \mathcal{L}^t, \mathcal{T}^t_u\right\}$ be a sequence generated by ELADMM Algorithm. Suppose that the sequence $\left\{\mathcal{A}^t, \mathcal{L}^t\right\}_{t=1}^{\infty}$ is bound. Then any accumulation point of the sequence $\left\{\mathcal{S}^t, \mathcal{A}^t, \mathcal{C}^t_u, \mathcal{L}^t, \mathcal{T}^t_u\right\}$ is a Karush-Kuhn-Tucker (KKT) point of the following optimization problem:

$$\min \sum_{u=1}^{3}\alpha_u \|\mathcal{C}_u\|_{\psi} + \lambda_1 \|\mathcal{L}\|_{\psi} + \lambda_2 \|\mathcal{S}\|_{\ell^{\psi}_{F,1}} + \beta f(\mathcal{A},\mathcal{L},\mathcal{S}), \quad \text{s.t. } \mathcal{C}_u = \nabla_u \mathcal{A},\ u \in [3].$$

Experiments & Results

Figure 1. Pseudo-color images of the four HSIs data sets.

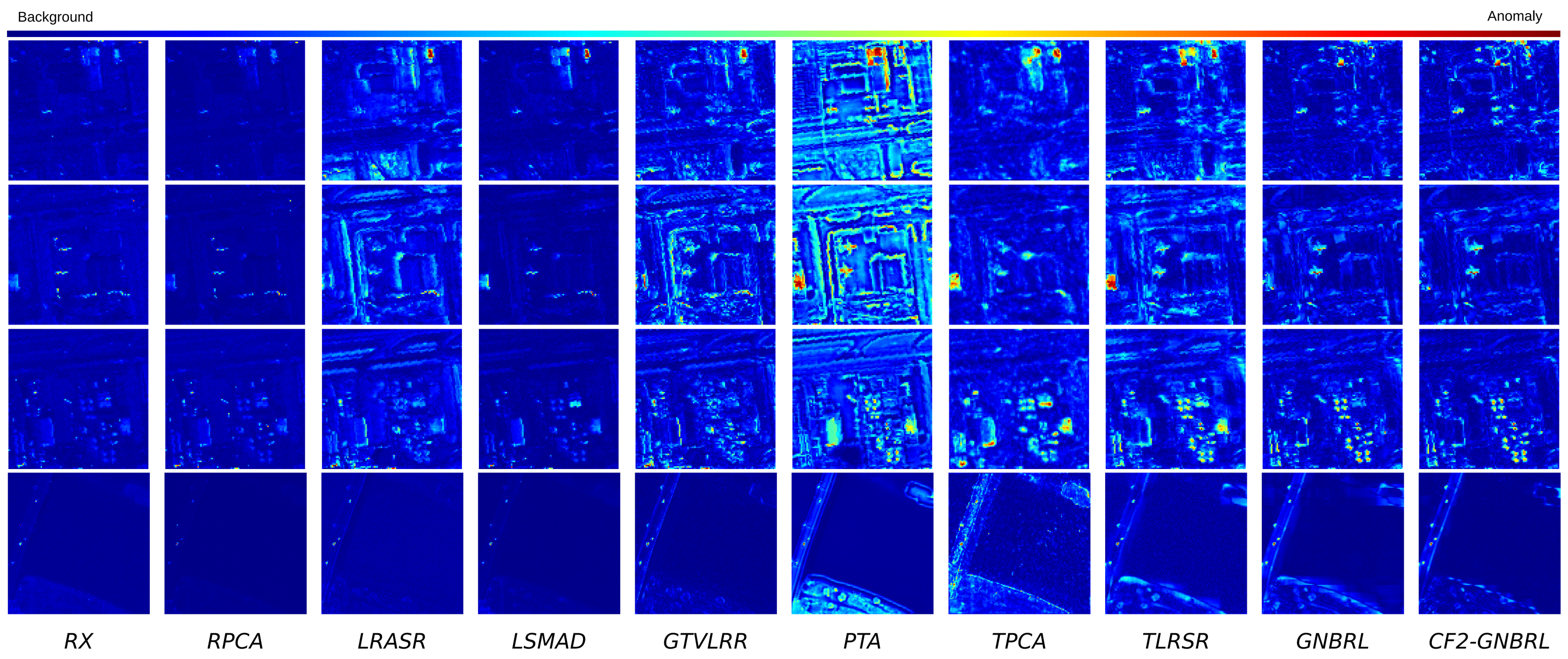

Figure 2. Target detection results by different methods for the four data sets.

HSI	Airport1		Airport2		Urban		Beach	
Algorithm	AUC (%)	Time (s)	AUC (%)	Time (s)	AUC (%)	Time (s)	AUC (%)	Time (s)
RX	82.21	0.42	84.03	0.41	96.92	0.41	95.39	0.04
RPCA	80.89	8.00	84.31	7.44	96.58	6.98	95.99	1.95
LRASR	77.28	53.81	86.48	70.13	92.89	47.51	95.65	104.90
LSMAD	83.39	9.54	92.17	8.60	96.05	8.74	97.06	7.65
GTVLRR	90.04	171.47	88.89	227.16	93.73	229.16	98.02	378.60
PTA	73.30	13.50	90.95	20.96	82.57	24.89	90.61	29.11
TPCA	80.22	30.91	88.90	30.62	93.69	22.15	95.82	21.71
TLRSR	90.56	3.44	94.57	3.63	97.10	3.58	95.98	5.84
GNBRL	94.75	1.60	98.00	1.50	98.38	1.91	98.03	4.01
CF2-GNBRL	**96.84**	27.14	**98.81**	31.63	**98.98**	31.40	**99.24**	83.06

Table 1. Comparison of AUC values (%) and running time (s) of different methods.

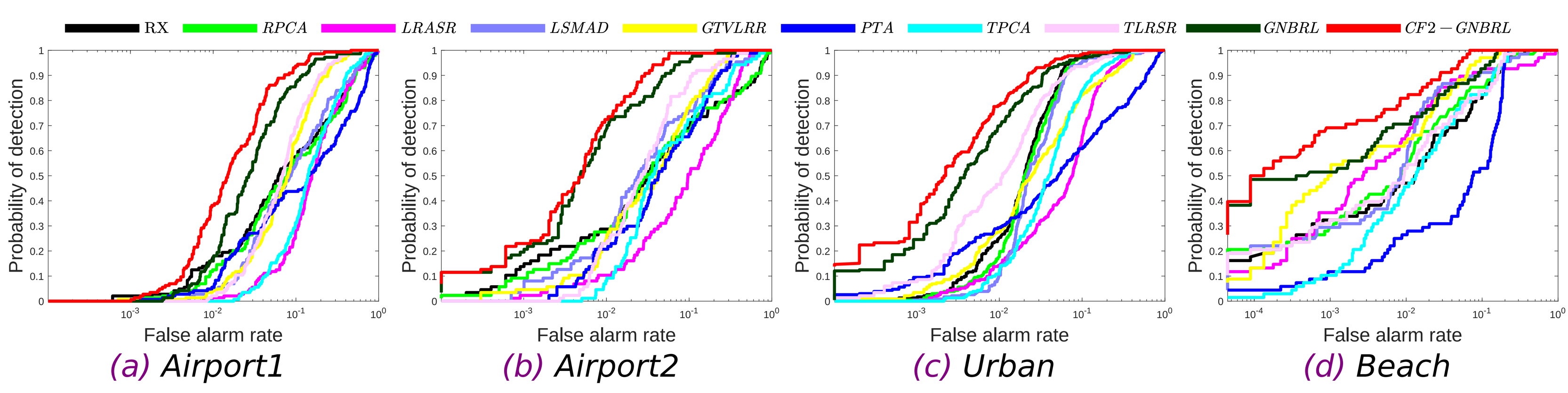

Figure 3. ROC curves obtained by different methods.

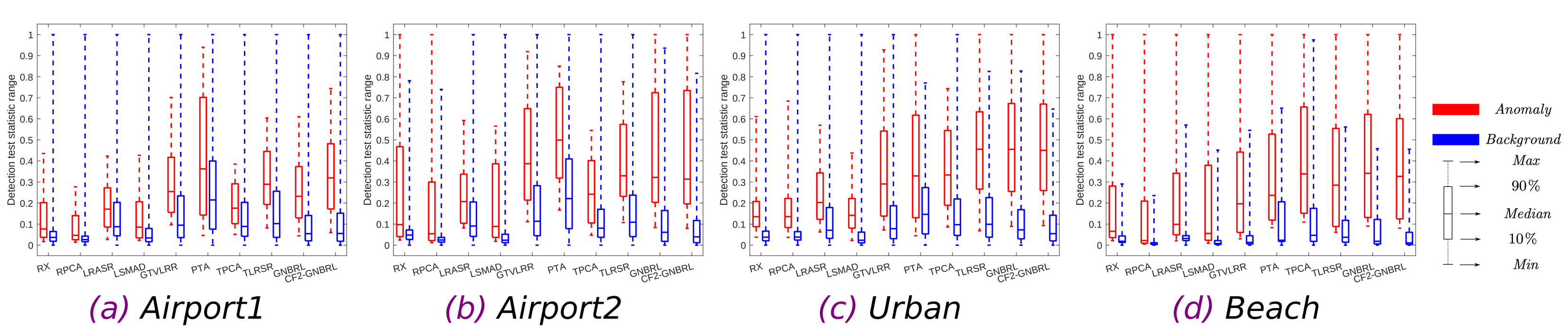

Figure 4. Separability maps of different methods.